Developmental Cell
Short Article

The Ordered Architecture of Murine Ear Epidermis Is Maintained by Progenitor Cells with Random Fate

David P. Doupé,[1] Allon M. Klein,[2,3] Benjamin D. Simons,[1,2] and Philip H. Jones[1,*]
[1]MRC Cancer Cell Unit, Hutchison-MRC Research Centre, Cambridge, CB2 0XZ, UK
[2]Cavendish Laboratory, Department of Physics, J.J. Thomson Avenue, University of Cambridge, Cambridge CB3 0HE, UK
[3]Department of Systems Biology, Harvard Medical School, 200 Longwood Avenue, Boston, MA 02115, USA
*Correspondence: phj20@cam.ac.uk
DOI 10.1016/j.devcel.2009.12.016

SUMMARY

Typical murine epidermis has a patterned structure, seen clearly in ear skin, with regular columns of differentiated cells overlying the proliferative basal layer. It has been proposed that each column is a clonal epidermal proliferative unit maintained by a central stem cell and its transit amplifying cell progeny. An alternative hypothesis is that proliferating basal cells have random fate, the probability of generating cycling or differentiated cells being balanced so homeostasis is achieved. The stochastic model seems irreconcilable with an ordered tissue. Here we use lineage tracing to reveal that basal cells generate clones with highly irregular shapes that contribute progeny to multiple columns. Basal cell fate and cell cycle time is random. Cell columns form due to the properties of postmitotic cells. We conclude that the ordered architecture of the epidermis is maintained by a stochastic progenitor cell population, providing a simple and robust mechanism of homeostasis.

INTRODUCTION

It has long been held that histological patterning reflects the organization and fate of the proliferating cells that maintain a given tissue (Allen and Potten, 1976; Mackenzie, 1970). One tissue thought to exemplify this principle is mammalian interfollicular epidermis (IFE), which consists of layers of keratinocytes that lie between hair follicles (Blanpain and Fuchs, 2009). The IFE is continually turned over: cells are shed from the epidermal surface and replaced by proliferating cells found in the basal cell layer. On commitment to terminal differentiation, basal cells exit the cell cycle and subsequently migrate into the suprabasal layers. At most body sites, the cells in the upper, cornified layers of the epidermis are arranged in regular columns (Allen and Potten, 1976; Mackenzie, 1970).

If one assumes that differentiated cells can only migrate vertically upwards on differentiation, it follows that each column must be maintained by the basal cells beneath it (Mackenzie, 1970). Following this argument, it has been hypothesized that the epidermis is arranged into clonal ''epidermal proliferative units'' or EPUs. Based on the observation that there were slightly fewer mitoses in basal cells lying beneath the center of the columns than in those at the periphery, it was proposed that a slow cycling stem cell lay at the center of each EPU (Potten, 1974). The stem cell generates an adjacent cluster of short lived transit amplifying (TA) cells that terminally differentiate after three rounds of cell division (Figures 1A and 1B) (Potten, 1974). The EPU model thus links tissue structure with the fate and spatial organization of stem and progenitor cells. This model has gained wide acceptance and continues to be used to interpret studies on homeostasis and carcinogenesis in the epidermis and other squamous epithelia of mice and humans (Croagh et al., 2008; Dotto, 2009; Ghazizadeh and Taichman, 2001, 2005; Ro and Rannala, 2005; Strachan and Ghadially, 2008; Zhang et al., 2001).

Recently an alternative model of epidermal homeostasis has been proposed based on quantitative lineage tracking in mouse tail epidermis (Clayton et al., 2007). This analysis revealed that all cycling basal cells (here termed committed progenitor or CP cells) are identical. CP cell division may have three possible outcomes, resulting in two proliferating cells, two postmitotic cells, or one proliferating and one postmitotic cell. These fates are adopted at random, but probabilities of the symmetric fates are balanced so that over the whole CP cell population, equal numbers of cycling and differentiating cells are produced, ensuring tissue homeostasis (Figure 1C) (Clayton et al., 2007; Jones and Simons, 2008). Although the CP model describes the expansion of clones in tail epidermis with precision, it is unclear if it applies to other areas of the epidermis, because the tail lacks the columns of cornified cells used to delineate EPU at other body sites (Allen and Potten, 1976; Potten, 1975; Spearman and Hardy, 1977).

In summary, the EPU model offers an account of homeostasis that uses the columnar arrangement of differentiated cells to infer the existence of clonal units in which stem and TA cell fate is predetermined. The implications of the stochastic CP paradigm for tissue organization have not been examined, and the issue of whether a tissue with a regular array of cell columns can be maintained by progenitors with random fate has not been resolved. We therefore investigated the relationship between the progenitor cell behavior and the columnar organization of IFE in the mouse ear where EPUs were first described, using quantitative genetic cell lineage tracing and 3D imaging (Mackenzie, 1970; Potten, 1974).

RESULTS AND DISCUSSION

Spatial Distribution of Proliferating and Differentiating Basal Cells

The EPU model asserts that approximately 10 basal cells are grouped beneath each column of cornified cells (Potten, 1974,

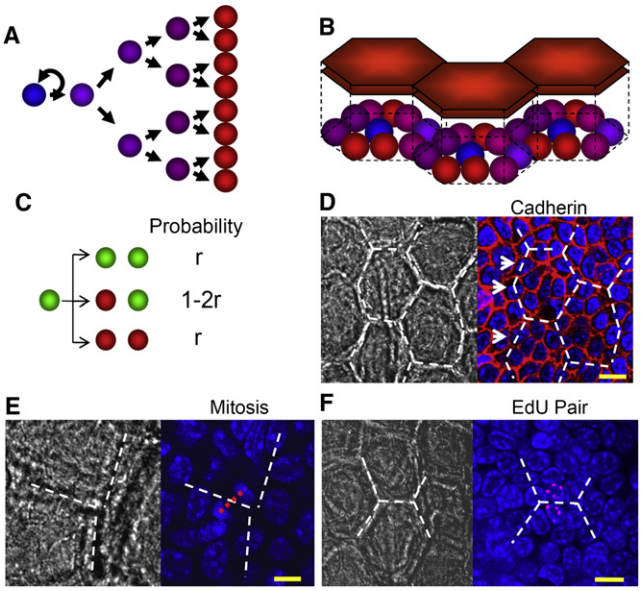

Figure 1. Models of Epidermal Homeostasis and Tissue Organization

(A) The stem/transit amplifying (TA) hypothesis. Long lived, slow cycling, self renewing stem cells (blue) generate a short lived population of TA cells (purple), which differentiate into postmitotic basal cells (red) after a limited number of cell divisions. Tissue maintenance requires the continual proliferation of stem cells.

(B) The epidermal proliferative unit (EPU) model. In ear epidermis, cornified cells (red hexagons) are arranged in columns. It has been proposed that the stem and TA cells are organized into discrete EPUs comprising a stem cell (blue), lying beneath the center of each column, which generates TA cells (purple) that in turn generate postmitotic cells (red circles), which leave the basal layer and migrate vertically upwards, differentiating into cornified cells.

(C) The committed progenitor (CP) cell model. All cycling basal cells (CP cells, green) are identical and may divide in one of three ways, generating two cycling daughters, two postmitotic daughters (red), or one cell of each type. Cell fate is random, but the probability of both types of symmetric division (r) is equal. An equal number of cycling and postmitotic cells are generated over the whole CP cell population to achieve homeostasis.

(D–F) Whole-mounts of ear epidermis were imaged by confocal microscopy. Left panels show the boundaries of cell columns (white dashed lines) in the cornified layer imaged by DIC; right panels show basal layer cells in the same samples. Scale bars (yellow) are 10 μm. (D) Samples stained for cadherin (red) and DAPI (blue) to detect cell borders: note that numerous basal cells cross the boundaries of the overlying cornified columns (white arrows). (E) Samples stained with DAPI (blue); red dotted line indicates a mitotic figure (identified by condensed chromatin from DAPI staining) spanning the border of adjacent cornified cell columns. (F) Samples stained for EdU (red) and DAPI (blue): animals were given a single injection of EdU 24 hr previously: pairs of EdU-positive cells result from the division of labeled cells. The cell pair shown crosses the boundary of adjacent cell columns. See also Figure S1.

1975). To investigate whether basal cells are arranged in this manner, we examined rendered confocal z stacks of whole-mounted mouse ear epidermis in which the cell columns could be clearly resolved by differential interference contrast (DIC) imaging and the underlying basal cells could be imaged by fluorescence (Figures 1D–1F). When the cell membranes of basal cells were visualized by cadherin staining, numerous cells were found to span the supposed EPU boundaries (Figure 1D). We then examined whether proliferation corresponded to the overlying cell columns. Mitotic figures were also found to span the projected boundaries of adjacent columns (Figure 1E). To exclude the possibility that basal cells "regroup" into EPU after mitosis, animals were given a single injection of the nucleotide analog EdU and were culled for analysis 24 hr later, by which time the cells labeled in S phase have divided to produce pairs of EdU-positive cells (Salic and Mitchison, 2008). Eleven of twenty-eight EdU-positive cell pairs crossed the boundaries of adjacent columns (Figure 1F). These results are at odds with the assertion that proliferating basal layer cells are organized into EPU.

A key observation that led to the development of the EPU model was that the frequency of mitoses was slightly lower in basal cells beneath the center of a cornified cell stack than for those at the periphery of the column. This difference was originally interpreted as indicating that there was a higher probability of differentiating, postmitotic, basal cells occupying central positions, but was later hypothesized to be due to the presence of a slow cycling stem cell in the central position of the EPU (Mackenzie, 1970; Potten, 1974). To investigate this question, we stained ear epidermal whole-mounts for keratin 10, a differentiation marker that is expressed in postmitotic basal and suprabasal cells (Braun et al., 2003) (see Figure S1 available online). The proportion of keratin-10-positive cells in central positions (29.4% ± 4.0%, mean ± SEM) was higher than that in the periphery (17.7% ± 2.7%) ($p = 0.02$, paired t test), suggesting that the difference in mitotic index may be due to an excess of differentiating cells beneath the center of the cornified cells rather than the presence of slow cycling stem cells.

Genetic Lineage Tracing

The results above appear to challenge the EPU model, but do not resolve how epidermal homeostasis is achieved. We therefore exploited inducible *cre*-lox based genetic marking to track the fate of a representative sample of proliferating cells and their progeny in adult mice (Clayton et al., 2007). The EPU model predicts that at late time points the only clones remaining in the basal layer will be those supported by a labeled stem cell and that clones will reach a constant upper size limit corresponding to an EPU. In contrast the CP model predicts three possible outcomes of cell division (Figure 1C), a wide range of clone sizes due to stochastic behavior, and that at late time points the clone size distribution will follow simple "scaling" behavior (i.e., the proportion of clones of size n at time t will be the same as that of clones size 2n at time 2t) (Clayton et al., 2007; Klein et al., 2007).

Cohorts of animals were induced at 8 or more weeks of age and culled for analysis at intervals from 3 days to 1 year. Cells expressing EYFP and their labeled progeny were detected by confocal microscopy of whole-mount epidermis.

We confirmed that the epidermis was in homeostasis during the experiment and that labeled clones were a representative sample of the proliferating cell population (see Supplemental Experimental Procedures, Figure S2A, and Tables S1 and S2). Crucially, at 1 year, clones included a representative percentage of cells lying beneath the center of cornified cell columns, the position predicted for stem cells according to the EPU model: 10.1% (39/349) of labeled cells were centrally located compared with 11.6% (45/343) of unlabeled cells (difference not significant by χ^2 test).

Following induction, cells were labeled at clonal density. The resulting clones were found to expand over time (Figure 2A).

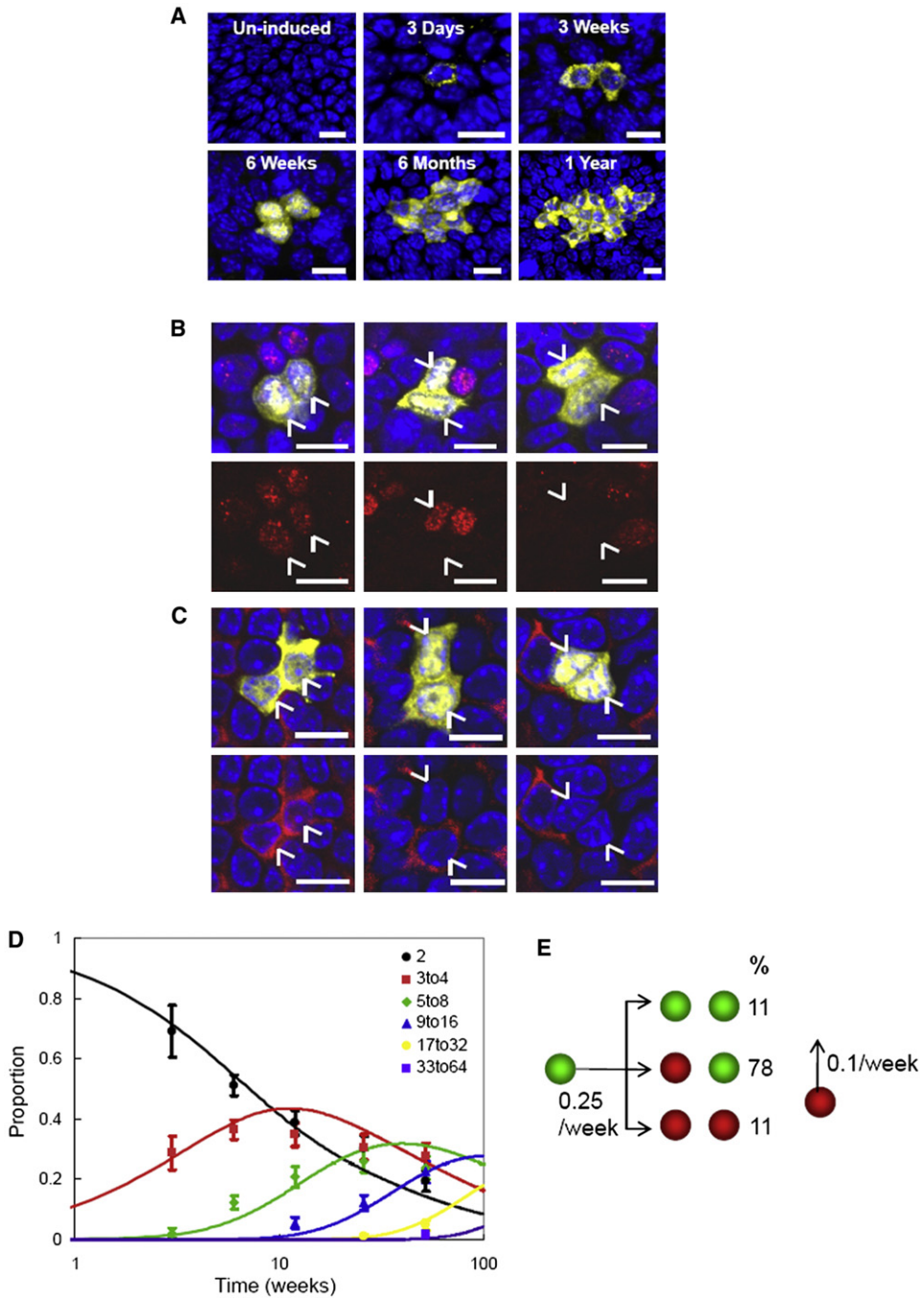

Figure 2. Clonal Fate and Division Outcomes

(A) Clonal labeling of proliferating cells. Rendered confocal z stack projections through the basal layer of typical clones at time points indicated following induction of EYFP by transient expression of a drug-regulated *cre* recombinase are shown. Yellow, EYFP; blue, DAPI nuclear stain. Scale bars, 10 μm.

(B and C) Fate of dividing basal cells. Two cell clones (6 weeks (B) or 3 months (C) postinduction, both cells in basal layer) show the possible fates of the daughters of a single cell division. Cells are stained for the proliferation marker Ki67 (B) or differentiation marker keratin 10 (C) (red). EYFP (yellow) and DAPI (blue); single slice confocal images are shown. Scale bar, 20 μm (B), 10 μm (C).

(D) Distribution of clone sizes (basal cells per clone) of clones containing two or more cells plotted against log time. Clone sizes are grouped in increasing powers of two as shown in the legend. Points with error bars (SEM) are clone fate data from an average of over 160 clones from three to five animals per time point. Curves indicate prediction of the model shown in (E).

(E) Ear epidermal homeostasis. Estimating the proportion of proliferating cells from Ki67 staining gives an average cycle time of 4 weeks, with cycling basal cells (green) dividing to generate cycling or postmitotic cells (red) with the probabilities (expressed as percentages) shown. On average postmitotic basal cells leave the basal layer by stratification every 10 weeks. See also Figure S2 and Tables S1 and S2.

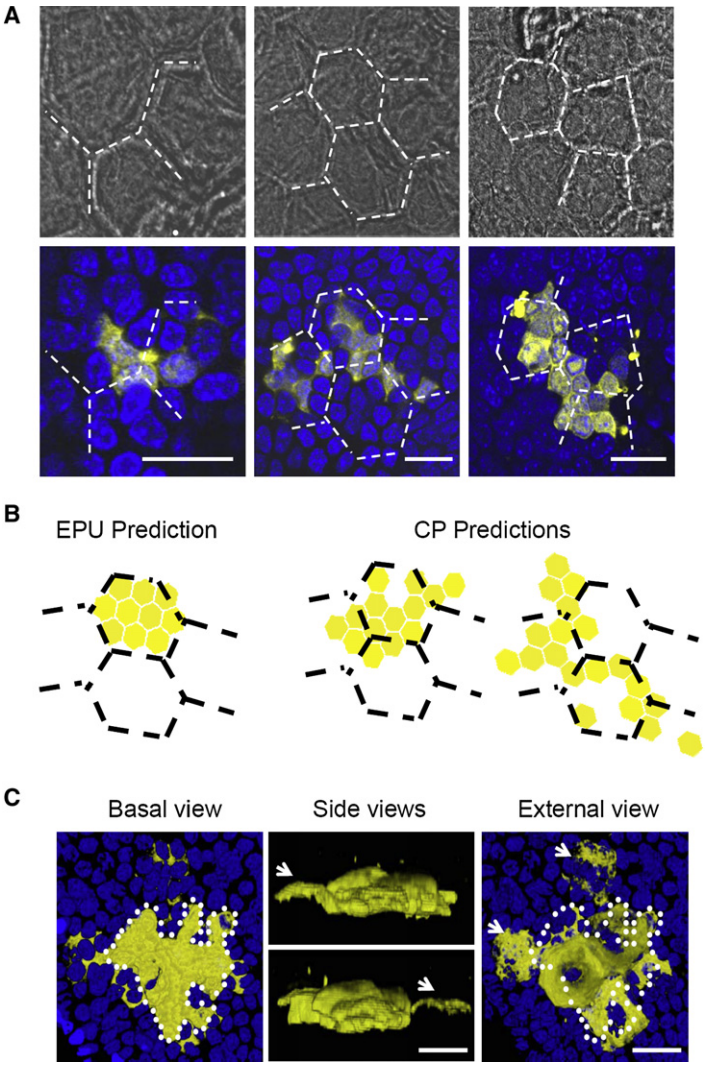

Figure 3. Clone Shape and Differentiation

(A) Clone shapes at 1 year. Single slice confocal images of the basal layer of typical 1 year clones (bottom panels) with corresponding DIC images (top panels) show the relationship between basal clone shape and columns of overlying squamous cells (dashed lines). Clones containing 3, 10, and 15 basal cells (left to right) all span multiple proposed EPUs in the basal layer without fully occupying any of them. Scale bars, 20 μm.

(B) Clone shape simulations. Left panel shows the prediction of the EPU model for clone shape in a genetic labeling experiment at a year after labeling. Only a clone supported by a labeled stem cell will persist and this will populate the EPU with labeled cells. Right panels show typical predicted clone shapes from a computer simulation using the model of cell behavior shown in Figure 2E (see Supplemental Experimental Procedures for details).

(C) Cornified cell columns in a 1 year clone. Projected z stack confocal images of a 1 year clone viewed from the basal surface (left panel), external surface (right panel), and the side (middle panels). Dotted line shows the basal layer footprint of the clone. Suprabasal cells extend beyond the bounds of the clone within the basal layer. Yellow, EYFP; blue, DAPI; scale bars, 20 μm. Arrows indicate labeled cornified cells interleaved in otherwise unlabeled cell columns.

Analysis of clones containing two basal cells revealed the three fates predicted by the CP model (Figures 2B and 2C), while at late time points the clone size distribution exhibits long time scaling (Figure S2C). Quantitative analysis demonstrates that the CP model provides an impressive fit to the entire clone size data set (Figures 2D, 2E, S2C, and S2D, and Supplemental Experimental Procedures). While previous lineage tracing studies have been interpreted within the EPU hypothesis, the data they present are qualitatively consistent with the CP model (Ghazizadeh and Taichman, 2001; Kameda et al., 2003; Mackenzie, 1997; Ro and Rannala, 2004, 2005).

CP Cell Fate Is Independent of the Overlying Cell Columns

The analysis above does not test the prediction of the EPU model that each column is clonal, i.e., supported by a progenitor cell that lies beneath it. To address if this is the case, we first analyzed the shape of clones at the 1 year time point. Rendered z stack confocal images of 63 unselected clones, in which the boundaries of the cornified cell stacks could be clearly visualized by DIC imaging, were examined. The basal layer "footprint" of 69% of these clones was smaller than a cornified cell, containing eight or fewer cells, but the majority (33/43) of these smaller clones crossed the boundary between adjacent overlying cell columns (Figure 3A). Fifteen percent of the clones contained nine to eleven cells, i.e., were of similar size to a cornified cell, but none of these were confined within the boundaries of a single cell column (Figure 3A). The remaining 16% of clones contained 12 or more cells: all of these clones cross the boundaries of at least three columns, and the largest clones span eight columns, but completely occupy none of them (Figure 3A). None of the clones examined fitted the EPU model prediction of a cluster of approximately 10 basal cells lying beneath a labeled stack of cornified cells. Furthermore, in a simple computer simulation of CP cells, we find an evolved range of clone shapes similar to that seen in vivo (Figure 3B, Supplemental Experimental Procedures).

Next we examined the fate of the differentiating cells in the clones. Labeled cornified cells were found interleaved with unlabeled cells in columns at the clone edge (Figure 3C). The cells within a single cornified cell column need not be derived from the basal cells directly beneath them and a single progenitor may contribute cells to multiple cell columns. We conclude that there is no relationship between the shape of clones in the basal layer and the overlying cell columns, and that the differentiated cells that make up each column are not clonal in origin.

CP Cell Cycle Time Is Stochastic

Given that the fate of CP cells is random, is there any regulation of the *timing* of cell division? It might be expected that cell cycle times are normally distributed about the average cell cycle time of one division every 4 weeks. However, such a distribution is inconsistent with the clone size data (see Supplemental

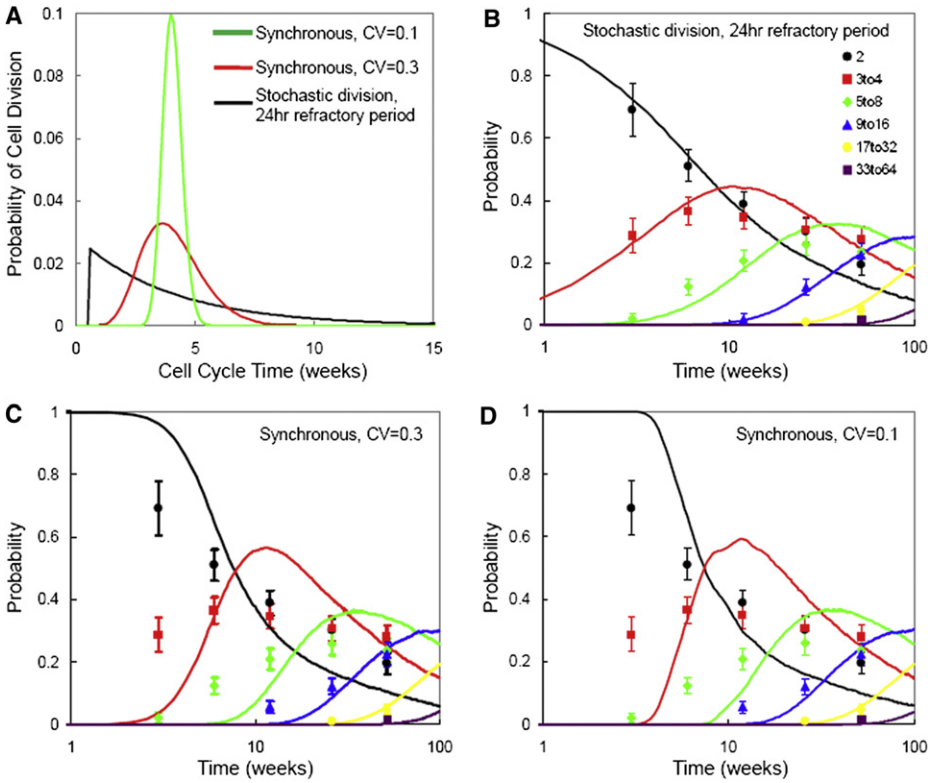

Figure 4. Cell Cycle Time Distribution in Proliferating Cells in Ear Epidermis

(A) Theoretical cell cycle time distributions about the average of 0.25/week. Synchronous cell divisions with a coefficient of variation of 0.1 (green line) and 0.3 (red line) are shown together with a distribution in which cell cycle time is random, with minimum cycle time of 24 hr (black line).

(B–D) Fit of the cell cycle distributions in (A) (solid lines) to the observed clone size data (points with error bars showing SEM, see Supplemental Experimental Procedures for details). The stochastic model fits the data well (B), while the synchronous models (C and D) cannot be reconciled with the observed clone size distributions.

Experimental Procedures and Figure 4). In contrast, a cell cycle time that is exponentially distributed (i.e., random) above a minimum period of ca. 24 hr fits the data with precision (Figure 4). It should be noted that the exact length of the minimum cell cycle time does not affect this conclusion. We conclude that for CP cells the time between cell divisions is random. Early cell kinetic studies with tritiated thymidine in ear epidermis and our own observations with EdU demonstrate that cells progress through S phase to mitosis within 24 hr of labeling, indicating that it is the length of G1 phase that varies stochastically (Pilgrim et al., 1966; Sherman et al., 1961). These results also explain the lack of a second peak in percent labeled mitosis studies of the epidermis (Potten et al., 1982).

The stochastic distribution of cell cycle times in the basal layer has important implications for label retaining cell (LRC) assays, which identify stem cells in some tissues (Braun and Watt, 2004). By chance a few CP cells may take over 10 weeks to divide (Figure 4A). Thus in ear epidermis, after a typical 70 day chase period, an LRC may be either a CP cell that has not divided by chance or a postmitotic cell generated by an asymmetric division of a labeled cell that has remained in the basal layer, rather than a slow cycling stem cell. LRC assays need to be interpreted with caution in tissues where cell fate and kinetics have not been defined.

Random Progenitor Cell Fate and Patterned Differentiation

We conclude that cells in the basal layer of the epidermis are not organized to support the overlying cell columns. All dividing cells in the basal layer are equivalent: their fate, their cell kinetics, and the spatial distribution of their progeny are random, but the probability of cells adopting a given fate is such that homeostasis is maintained. Such balanced ''population asymmetry'' offers a robust means of supporting homeostasis, because the death of an individual CP cell has little impact (Watt and Hogan, 2000). In contrast, if the tissue is arranged in proliferative units, the loss of a single stem cell removes an entire clonal unit. The regulation of proliferation in the basal layer may be achieved simply by contact inhibition. CP cells only divide when a nearby postmitotic cell stratifies out of the basal layer, so the rates of stratification and proliferation are directly linked. This enables the tissue to respond to an increased requirement for differentiated cells without the complex regulation of stem and TA cells with preset fate envisaged in the EPU paradigm.

These results exclude the existence of a discrete population of slow cycling, long lived, self renewing stem cells in ear epidermis representing 10% of basal cells as proposed in the EPU hypothesis (Potten, 1974, 1975). Furthermore, while we cannot completely exclude a very rare population of such cells, the data

show even if present such cells make no detectable contribution to homeostasis in this sample of over 800 clones. At other epidermal body sites it has been demonstrated that wounding activates hair follicle stem cells whose progeny do not normally contribute to interfollicular epidermis (Ito et al., 2005; Levy et al., 2005, 2007). It will be interesting to study how the ear epidermis responds to challenges such as wounding.

If the behavior of cells is random, how do the columns of differentiated cells form? A possible explanation lies in the shape and size of cornified layer cells. The shape of the cornified cells alone results in their packing together in regular columns (Menton, 1976a, 1976b). In simulations, cornified cell columns form even when differentiating cells leave the basal layer at random (Honda and Oshibe, 1984; Honda et al., 1996). Furthermore, as each cornified column covers about 10 basal cells, local fluctuations in the rate of stratification of basal cells will be averaged out. The formation of differentiated cell columns in the epidermis is thus a robust, self organizing process, independent of the basal layer. The columns result from the morphology of the cornified cells. It seems likely that similar principles apply in other tissues: patterning of differentiated cells should not be assumed to reflect proliferative organization and deterministic models of cell fate.

EXPERIMENTAL PROCEDURES

Adult mice doubly transgenic for the inducible *cre* allele AhcreERT and the conditional reporter allele of EYFP targeted to the Rosa 26 locus were generated as described (Clayton et al., 2007; Kemp et al., 2004; Srinivas et al., 2001). EYFP expression was induced in animals of at least 8 weeks of age as described by one or two intraperitoneal doses of 80 mg/kg β-napthoflavone and 1 mg tamoxifen (Clayton et al., 2007). At time points stated in the text, after induction, cohorts were culled for analysis. For EdU experiments a single intraperitoneal dose of 0.1 mg EdU in PBS was given at time stated prior to culling. All experiments were conducted according to Home Office project license PPL80/2056.

Whole-mounts of ear epidermis were prepared as described (Braun et al., 2003). Briefly, ears were cut into 5 mm squares and incubated for 3 hr in 5 mM EDTA at 37°C. The epidermis was then carefully peeled away with fine forceps and fixed in 4% paraformaldehyde for 45 min.

For staining, whole-mounts were blocked for 1 hr in buffer (0.5% Bovine Serum Albumen, 0.25% Fish skin gelatin, and 0.5% Triton X-100 in PBS) with 10% donkey or goat serum (according to the secondary antibody used). Primary and secondary antibodies were incubated in buffer overnight, followed by washing for 4 hr with 0.2% Tween20 in PBS. Antibodies used were as follows: chicken anti-GFP (Invitrogen A10262); rabbit anti Ki67 (Abcam, ab16667); rabbit anti keratin 10 (Covance PRB159P); and goat anti-pan-cadherin (Santa Cruz sc1499). Alexa Fluor secondary antibodies from Invitrogen were used. EdU incorporation was detected with a Click chemistry kit according to the manufacturer's instructions (Invitrogen).

SUPPLEMENTAL INFORMATION

Supplemental Information for this article includes two figures, two tables, Supplemental Experimental Procedures, and Supplemental Results and can be found with this article online at doi:10.1016/j.devcel.2009.12.016.

ACKNOWLEDGMENTS

We thank Esther Choolun for expert technical assistance and the MRC, the EPSRC, the National Centre for the Replacement, Refinement and Reduction of Animals in Research, and Sidney Sussex College, Cambridge for funding.

Received: August 21, 2009
Revised: November 27, 2009
Accepted: December 16, 2009
Published: February 15, 2010

REFERENCES

Allen, T.D., and Potten, C.S. (1976). Significance of cell shape in tissue architecture. Nature *264*, 545–547.

Blanpain, C., and Fuchs, E. (2009). Epidermal homeostasis: a balancing act of stem cells in the skin. Nat. Rev. Mol. Cell Biol. *10*, 207–217.

Braun, K.M., and Watt, F.M. (2004). Epidermal label-retaining cells: background and recent applications. J. Investig. Dermatol. Symp. Proc. *9*, 196–201.

Braun, K.M., Niemann, C., Jensen, U.B., Sundberg, J.P., Silva-Vargas, V., and Watt, F.M. (2003). Manipulation of stem cell proliferation and lineage commitment: visualisation of label-retaining cells in wholemounts of mouse epidermis. Development *130*, 5241–5255.

Clayton, E., Doupe, D.P., Klein, A.M., Winton, D.J., Simons, B.D., and Jones, P.H. (2007). A single type of progenitor cell maintains normal epidermis. Nature *446*, 185–189.

Croagh, D., Thomas, R.J., Phillips, W.A., and Kaur, P. (2008). Esophageal stem cells–a review of their identification and characterization. Stem Cell Rev. *4*, 261–268.

Dotto, G.P. (2009). Crosstalk of Notch with p53 and p63 in cancer growth control. Nat. Rev. Cancer *9*, 587–595.

Ghazizadeh, S., and Taichman, L.B. (2001). Multiple classes of stem cells in cutaneous epithelium: a lineage analysis of adult mouse skin. EMBO J. *20*, 1215–1222.

Ghazizadeh, S., and Taichman, L.B. (2005). Organization of stem cells and their progeny in human epidermis. J. Invest. Dermatol. *124*, 367–372.

Honda, H., and Oshibe, S. (1984). A computer simulation of cell stacking for even thickness in mammalian epidermis. J. Theor. Biol. *111*, 625–633.

Honda, H., Tanemura, M., and Imayama, S. (1996). Spontaneous architectural organization of mammalian epidermis from random cell packing. J. Invest. Dermatol. *106*, 312–315.

Ito, M., Liu, Y., Yang, Z., Nguyen, J., Liang, F., Morris, R.J., and Cotsarelis, G. (2005). Stem cells in the hair follicle bulge contribute to wound repair but not to homeostasis of the epidermis. Nat. Med. *11*, 1351–1354.

Jones, P., and Simons, B.D. (2008). Epidermal homeostasis: do committed progenitors work while stem cells sleep? Nat. Rev. Mol. Cell Biol. *9*, 82–88.

Kameda, T., Nakata, A., Mizutani, T., Terada, K., Iba, H., and Sugiyama, T. (2003). Analysis of the cellular heterogeneity in the basal layer of mouse ear epidermis: an approach from partial decomposition in vitro and retroviral cell marking in vivo. Exp. Cell Res. *283*, 167–183.

Kemp, R., Ireland, H., Clayton, E., Houghton, C., Howard, L., and Winton, D.J. (2004). Elimination of background recombination: somatic induction of Cre by combined transcriptional regulation and hormone binding affinity. Nucleic Acids Res. *32*, e92.

Klein, A.M., Doupe, D.P., Jones, P.H., and Simons, B.D. (2007). Kinetics of cell division in epidermal maintenance. Phys. Rev. E Stat. Nonlin. Soft Matter Phys. *76*, 021910.

Levy, V., Lindon, C., Harfe, B.D., and Morgan, B.A. (2005). Distinct stem cell populations regenerate the follicle and interfollicular epidermis. Dev. Cell *9*, 855–861.

Levy, V., Lindon, C., Zheng, Y., Harfe, B.D., and Morgan, B.A. (2007). Epidermal stem cells arise from the hair follicle after wounding. FASEB J. *21*, 1358–1366.

Mackenzie, I.C. (1970). Relationship between mitosis and the ordered structure of the stratum corneum in mouse epidermis. Nature *226*, 653–655.

Mackenzie, I.C. (1997). Retroviral transduction of murine epidermal stem cells demonstrates clonal units of epidermal structure. J. Invest. Dermatol. *109*, 377–383.

Menton, D.N. (1976a). A liquid film model of tetrakaidecahedral packing to account for the establishment of epidermal cell columns. J. Invest. Dermatol. *66*, 283–291.

Menton, D.N. (1976b). A minimum-surface mechanism to account for the organization of cells into columns in the mammalian epidermis. Am. J. Anat. *145*, 1–22.

Pilgrim, C., Lang, W., and Maurer, W. (1966). Exp. Cell Res. *44*, 129–138.

Potten, C.S. (1974). The epidermal proliferative unit: the possible role of the central basal cell. Cell Tissue Kinet. *7*, 77–88.

Potten, C.S. (1975). Epidermal cell production rates. J. Invest. Dermatol. *65*, 488–500.

Potten, C.S., Wichmann, H.E., Loeffler, M., Dobek, K., and Major, D. (1982). Evidence for discrete cell kinetic subpopulations in mouse epidermis based on mathematical analysis. Cell Tissue Kinet. *15*, 305–329.

Ro, S., and Rannala, B. (2004). A stop-EGFP transgenic mouse to detect clonal cell lineages generated by mutation. EMBO Rep. *5*, 914–920.

Ro, S., and Rannala, B. (2005). Evidence from the stop-EGFP mouse supports a niche-sharing model of epidermal proliferative units. Exp. Dermatol. *14*, 838–843.

Salic, A., and Mitchison, T.J. (2008). A chemical method for fast and sensitive detection of DNA synthesis in vivo. Proc. Natl. Acad. Sci. USA *105*, 2415–2420.

Sherman, F.G., Quastler, H., and Wimber, D.R. (1961). Cell population kinetics in the ear epidermis of mice. Exp. Cell Res. *25*, 114–119.

Spearman, R.I., and Hardy, J.A. (1977). Ultrastructure of the contrasting types of keratinization seen in the tail epidermis of the laboratory mouse Mus musculus. Arch. Dermatol. Res. *258*, 33–40.

Srinivas, S., Watanabe, T., Lin, C.S., William, C.M., Tanabe, Y., Jessell, T.M., and Costantini, F. (2001). Cre reporter strains produced by targeted insertion of EYFP and ECFP into the ROSA26 locus. BMC Dev. Biol. *1*, 4.

Strachan, L.R., and Ghadially, R. (2008). Tiers of clonal organization in the epidermis: the epidermal proliferation unit revisited. Stem Cell Rev. *4*, 149–157.

Watt, F.M., and Hogan, B.L. (2000). Out of Eden: stem cells and their niches. Science *287*, 1427–1430.

Zhang, W., Remenyik, E., Zelterman, D., Brash, D.E., and Wikonkal, N.M. (2001). Escaping the stem cell compartment: sustained UVB exposure allows p53-mutant keratinocytes to colonize adjacent epidermal proliferating units without incurring additional mutations. Proc. Natl. Acad. Sci. USA *98*, 13948–13953.